Ultrastructural Characterization of the Implant Interface Response to Loading

1. X. Zhang[1,2]
2. J. Duyck[1]
3. K. Vandamme[1]
4. I. Naert[1]
5. G. Carmeliet[3,*]

[1]*Department of Oral Health Sciences, BIOMAT Research Cluster & Prosthetic Dentistry, KU Leuven & University Hospitals Leuven, Leuven, Belgium*
[2]*Guanghua School of Stomatology, Hospital of Stomatology, Sun Yat-sen University, Guangzhou, China*
[3]*Department of Clinical and Experimental Medicine, Clinical and Experimental Endocrinology, KU Leuven, O&N I Herestraat 49 - Box 902, 3000 Leuven, Belgium*

1. ↵* geert.carmeliet@med.kuleuven.be

Abstract

Dynamic loading can affect the bone surrounding implants. For ultrastructural exploration of the peri-implant tissue response to dynamic loading, titanium implants were installed in rat tibiae, in which one implant was loaded while the contralateral served as the unloaded control. The loaded implants received stimulation either within 24 hrs after implantation (immediate loading) or after a 28-day healing period (delayed loading) for 4, 7, 14, 21, or 28 days. The samples were processed for histology and gene expression quantification. Compared with the unloaded control, bone-to-implant contact increased significantly by immediate loading for 28 days ($p < .05$), but not in case of delayed loading. No effect of loading was observed on the bone formation in the implant thread areas, on the blood vessel area, and on endosteal callus formation. Loading during healing (immediate) for 7 days induced, relative to the unloaded control, a 2.3-fold increase of *Runx2* in peri-implant cortical bone ($p < .01$) without a change in the *RANKL/Opg* ratio. Loading after healing (delayed) for 7 days up-regulated *Runx2* (4.3-fold, $p < .01$) as well as *Opg* (22.3-fold, $p < .05$) compared with the unloaded control, resulting in a significantly decreased *RANKL/Opg* ratio. These results indicate a stimulating effect of dynamic loading on implant osseointegration when applied during the healing phase. In addition, gene expression analyses revealed molecular adaptations favoring bone formation and, at the same time, affecting bone remodeling.

Introduction

Loading of implants during their healing phase ('immediate loading') is prevalent in clinics today. Evidence has been provided, *via* animal experiments, that dynamic immediate loading can stimulate and improve implant osseointegration (De Smet *et al.*, 2005; Duyck *et al.*, 2006, 2007; Vandamme *et al.*, 2007, 2008). High success rates for the immediate loading protocol have been reported in clinical studies (Esposito *et al.*, 2009; Mertens and Steveling, 2011). However, this clinical outcome has thus far been evidenced exclusively in studies with well-defined situations, with selected patients, and with relatively short-term follow-up periods. Therefore, data on immediate loading

of implants are encouraging, but still far from optimal (Esposito *et al.*, 2009). Thorough insight into tissue responses to implant loading during and after osseointegration is still limited, although required for scientific support of the clinical shift from delayed to immediate loading protocols. The aim of the present study was to evaluate the peri-implant bone response to immediate and delayed implant loading at tissue, cellular, and molecular levels. The study hypothesis was two-fold: (i) Controlled implant loading enhances osseointegration, and (ii) the peri-implant tissue response to loading depends on the timing of load application.

Materials & Methods

Animals and Implants

Male Wistar rats (*Janvier*, Paris, France; n = 130) with a body weight of 364 ± 17 g were distributed over 10 groups, differing in loading protocol (immediate loading, delayed loading) and experimental duration (4, 7, 14, 21, and 28 days). Implants and surgery are described in online Appendix A.

Mechanical Loading

Implant loading was performed as previously described (De Smet *et al.*, 2005, 2006; Slaets *et al.*, 2009). For each animal, one tibia was randomly selected to harbor the implant that was loaded, while the contralateral one served as the unloaded control. For the immediate loading protocol, the loading started within 24 hrs following surgery. For delayed loading, a 28-day healing time prior to loading was respected. Loading was applied for 4, 7, 14, 21, or 28 days. The loading parameters applied were chosen based on previous *ex vivo* strain gauge measurements, indicating the osteogenic potential of these parameters (De Smet *et al.*, 2005, 2006; Slaets *et al.*, 2009). The protocol of the animal experiment was approved by the ethical committee of KU Leuven (P029/2008), complied with ARRIVE guidelines for pre-clinical studies, and was performed according to Belgian animal welfare regulations and guidelines.

Tissue and Cellular Analysis

Resin-embedded samples were used for assessment of implant osseointegration (BIC), paraffin-embedded samples for quantification of peri-implant bone formation and remodeling (BA), tissue vascularization (VA), and callus formation (C.Ar/T.Ar) and composition (B.Ar/C.Ar) in the bone marrow region (Fig. 1). Animal and sample grouping relative to the loading regime and processing type and histomorphometric assessments are detailed in online Appendix A.

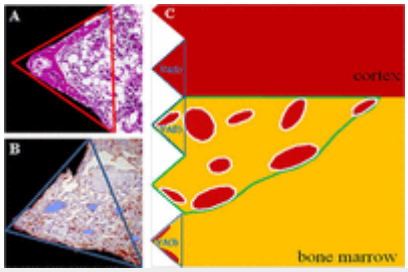

Figure 1.

Illustrations of the quantitative measurements performed on paraffin-embedded implant-bone samples. **(A)** In the peri-implant region at bone marrow level, the bone tissue present in the implant V-threads (red-outlined triangular area) was calculated and allocated to a quartile category (Bone area - BA; score 1, 2, 3, or 4 for 0% to 25%, 25% to 50%, 50% to 75%, and 75% to 100%, respectively). **(B)** The blood vessel area (VA, %) was quantified in 3 regions by the ratio of

the vessel surface area (highlighted in blue) to the tissue surface area (blue-outlined area). (C) Axisymmetric schematic representation of the 3 different regions where tissue vascularization (VA) was determined and of the quantification of the endosteal callus size and its bone content. A tissue area (T.Ar) was defined encompassing the bone marrow region between the medial and lateral cortex, and extending up to a distance of 1,500 μm from the implant surface. The size of the endosteal callus (C.Ar/T.Ar, %) was quantified by measurement of the total area of the endosteal callus (green line) relative to the tissue area. The bone content of the endosteal callus (B.Ar/C.Ar, %) was defined as the bone area (white-outlined bone spicules) relative to the total area of the endosteal callus (green line).

Molecular Analysis

Expression of genes in response to seven-day loading was investigated in bone tissue originating from the medial peri-implant cortex (*i.e.*, the top part of the implant). The cortical bone around the implant neck was biopsied and snap-frozen in liquid nitrogen. Standard procedures for qPCR analysis were carried out (see online Appendix A). The mRNA expression of selected bone-formation-related (*Runx2, Col1a1, Opn, Oc*) and bone-resorption-related (*RANKL, Opg, Ctsk*) genes was analyzed.

Statistical Analysis

One-/two-way analysis of variance (ANOVA) followed by Tukey's HSD test (SPSS, Chicago, IL, USA) was performed for assessment of the effects of loading and of the duration of the experimental period on the peri-implant tissue responses. Any p values $< .05$ were considered significant.

Results

Histological Observations

Histology revealed a similar bone repair pattern for both loaded and unloaded implants. Furthermore, differences in bone composition and architecture were noticed between the groups with implant healing time up to 28 days and up to 56 days. Both new bone formation and bone remodeling were perceived in the peri-implant tissues of the former groups. At the peri-implant cortex, bone apposition from the host bone toward the implant as well as bone remodeling in the cortex were observed. In the peri-implant medullar region, callus woven bone was observed, originating from the endosteum and extending along the implant surface. Over time, this newly formed bone was remodeled into denser, lamellar bone. For the groups where delayed loading/unloading was applied, signs of remodeling were noticed but without obvious changes in the cortical bone adjacent to the implant. In the peri-implant medullar region, dense bone was noticed in close contact with the implant and was found to remain stable over time.

Implant Osseointegration

Compared with the unloaded control, an increased BIC was induced by 28-day loading in the immediate loading regime (77.67% ± 2.17% *vs.* 65.71% ± 3.49%, loaded *vs.* unloaded, $p < .05$), while no significant effect of loading on BIC was observed for delayed loaded implants (75.91% ± 6.71% *vs.* 76.1% ± 5.67%, loaded *vs.* unloaded).

Bone Formation and Vascularization in the Implant V-thread Areas

Compared with the unloaded control, loading did not display a manifest effect on the bone formation (BA) in the implant V-thread areas. The duration of experimental loading/unloading

(corresponding to the healing time of the interfacial tissues), however, significantly affected BA (ANOVA; see online Appendix B). In the immediate loading regime, an overall increase of the BA score from day 4 to day 28 was observed (Fig. 2A). *Post hoc* tests investigating the differences between BA at the different observation points revealed a significantly lower BA after 4 days of loaded/unloaded healing compared with all the other time points ($p < .01$). Further selected significant BA increases in response to the duration of the experiment were recorded. In the delayed loading regime, a different BA kinetic pattern was observed between the unloaded and the loaded conditions (Fig. 2B). For the unloaded implants, a gradual increase of BA from day 7 onward could be seen. For the loaded implants, BA also increased from day 7 and peaked at 21 days. *Post hoc* analyses demonstrated significantly lower BA at 4 days compared with 21 and 28 days, and at 7 days compared with 21 and 28 days of loaded/unloaded healing ($p < .01$ for all comparisons).

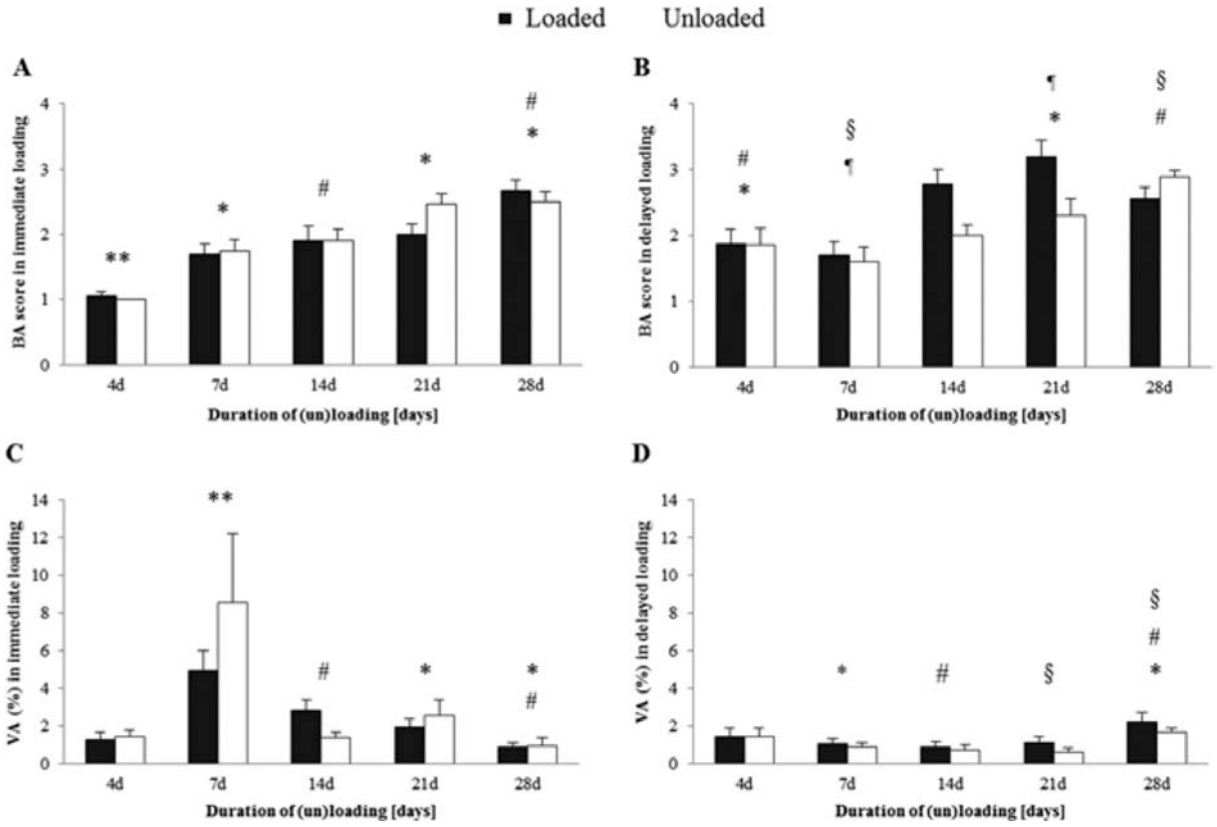

Figure 2.

Bone formation and vascularization in the implant V-thread areas. **(A, B)** Mechanical and temporal changes in the peri-implant bone formation. The bone area (BA) was scored in the V-thread area in the medullar region of loaded (black bars) and unloaded (white bars) samples of the immediate (A) or delayed (B) loading regime. **(C, D)** Mechanical and temporal changes in the peri-implant vascularization. The blood vessel area (VA, %) was measured in the first V-thread area beneath the cortex [VA(2)] on CD31-stained sections of loaded (black bars) and unloaded (white bars) samples of the immediate (C) or delayed (D) loading regimen. Means and standard errors of the mean are shown. Identical symbols refer to a significant difference between the time points regardless of loaded or unloaded condition. A double asterisk (**) indicates a significant difference from all other time points (2-way ANOVA and *post hoc* Tukey HSD tests with $p < .05$).

Tissue vascularization was unaffected by loading for all 3 defined V-thread areas (ANOVA; see online Appendix B). Conversely, the vascularization in the 1st V-thread tissue beneath the cortex (VA2) changed significantly over time (ANOVA; $p < .01$) with a specific pattern depending on the loading regime (see online Appendix B). In the immediate loading regime, VA increased from day 4 onward, reached its peak on day 7, and then gradually decreased until day 28 (Fig. 2C). In the delayed loading regime, VA remained stable at all observation time points with the exception of day 28, where an increase was noticed compared with days 7, 14, and 21 (Fig. 2D). The results of the *post hoc* analyses exploring differences between the time points within a loading regime are indicated in Figs. 2C and 2D. Of note, the vascularization of the tissues healed up to 28 days (group of unloaded and immediate loaded implants) was manifestly higher than the vascularization of the samples analyzed after 28 days up to 56 days of healing [delayed (un)loading groups].

Callus and Bone Formation in the Peri-implant Endosteal and Bone Marrow Region

No loading effect on the size of the callus (C.Ar/T.Ar) and its bone content (B.Ar/C.Ar) was found in either the immediate or delayed loading regime (ANOVA; online Appendix B). A time-dependent increase in C.Ar/T.Ar was observed after 28 days in the immediate loading regime, significantly different from the preceding observation point of 21 days ($p < .01$) (Fig. 3A). In addition, a progressive increase in the amount of bone matrix in the callus (B.Ar/C.Ar) was clearly noticed in case of immediate loading, resulting in significantly higher bone content from day 14 onward compared with the earlier time points ($p < .05$) (Fig. 3B). The results of the *post hoc* analyses exploring differences between the time points for the immediate loading regime for C.Ar/T.Ar and for B.Ar/C.Ar are indicated in Figs. 3A and 3B, respectively. These temporal changes in callus area and bone content were not detected in the delayed loading regime (Figs. 3C, 3D).

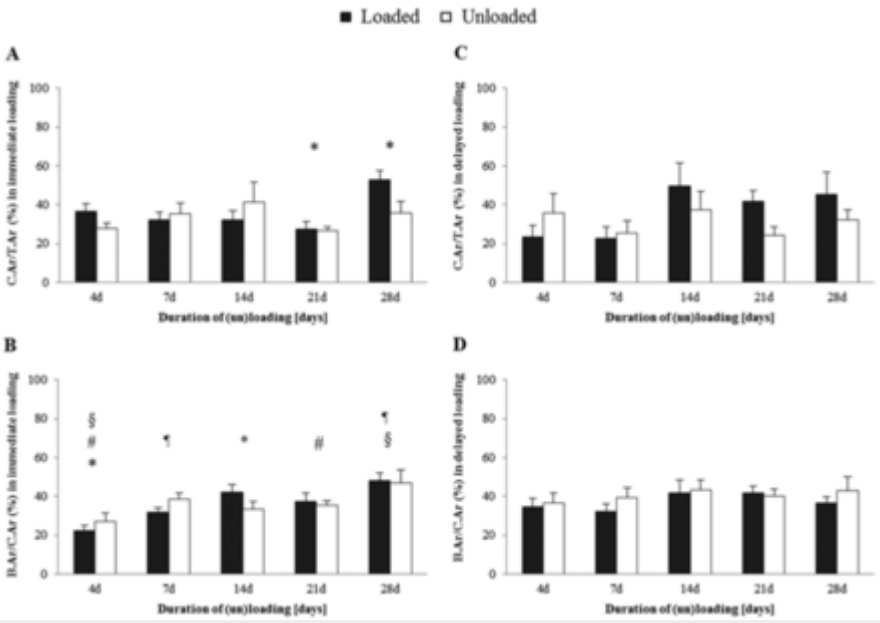

Figure 3.

Callus formation (C.Ar/T.Ar, %) and its bone content (B.Ar/C.Ar, %) was measured on H&E-stained sections of loaded (black bars) and unloaded (white bars) samples originating from immediate and delayed loading regimes. Means and standard errors of the mean are shown. Identical symbols refer to a significant difference over time (2-way ANOVA and *post hoc* Tukey HSD tests with $p < .01$).

Gene Expressions in the Peri-implant Cortical Bone Tissue

The average RNA yield was 53.95 (± 4.94) μg *per* explant. Immediate loading led to a significantly increased *Runx2* expression compared with that in the unloaded control (2.3-fold increase; $p < .01$) (Fig. 4A). No differences in the expression of the other bone markers were observed. Similarly, delayed loading resulted in an increase of *Runx2* (4.3-fold; $p < .01$). Additionally, a 22.3-fold enhancement of *Opg* ($p < .05$) (Fig. 4B) and an significant accompanying decrease of the *RANKL/Opg* ratio in response to delayed loading were found, when compared with the unloaded control ($p < .01$).

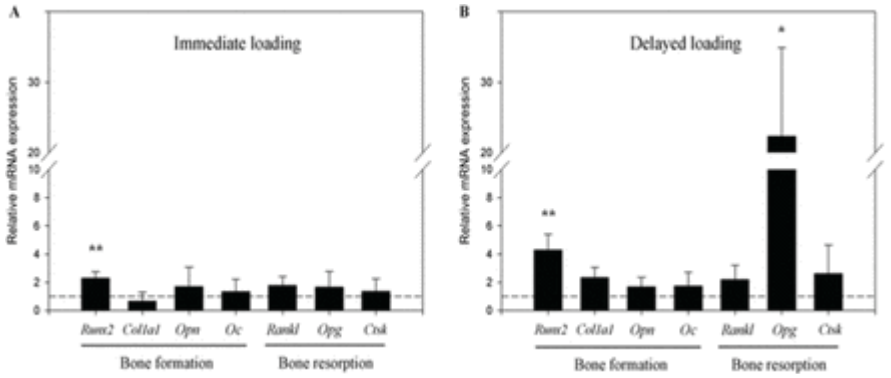

Figure 4.

Gene expression in the peri-implant cortical bone. Quantitative real-time PCR analysis of the expression of selected genes involved in bone formation and bone resorption in response to 7 days of immediate **(A)** and delayed **(B)** loading (dotted line, normalized to unloaded control; $*p < .05$ and $**p < .01$ compared with the normalized control; 1-way ANOVA).

Discussion

The peri-implant tissue response to well-controlled loading was investigated based on the hypotheses that (i) controlled implant loading enhances osseointegration and that (ii) the type and extent of the peri-implant tissue response to loading depend on the timing of load application. These hypotheses could be only partly confirmed: Controlled implant loading stimulated osseointegration but exclusively when applied during the implant healing phase (immediate loading). A significant effect of loading on tissue and cellular adaptations in the peri-implant region could not be detected by the assays used. In contrast, molecular analysis of the peri-implant cortical bone revealed a differential expression of the osteoblast-/osteoclast-related genes for the 2 loading protocols.

Applied immediate implant loading enhanced implant osseointegration, in line with previous findings (De Smet *et al.*, 2005; Duyck *et al.*, 2006, 2007; Vandamme *et al.*, 2007, 2008). The absence of an effect of loading on implant osseointegration when applied at the later healing stage corroborates available data (Sasaki *et al.*, 2008; Wiskott *et al.*, 2008). Furthermore, the implants that were immediately loaded attained a degree of osseointegration similar to that of the implants that received delayed loading or that were left to heal for 56 days without being loaded. In this respect, we could state that immediate loading accelerated implant osseointegration. However, BIC data at earlier time points are lacking, thereby precluding the assessment of the impact of immediate loading on the onset and extent of osseointegration.

Regarding the bone content of the implant tissue spikes, no significant loading effect could be observed. A temporal increase in bone area, however, was clearly present, and this finding is

consistent with results from previous studies in rabbits (Slaets *et al.*, 2006, 2007). Conversely, an increase in peri-implant bone density induced by delayed loading has also been reported (Wiskott *et al.*, 2008), indicating that well-organized, mature peri-implant bone can be triggered to adapt to an altered biomechanical challenge. The discrepancy between the latter report and our results is likely due to the applied loading protocol and the experimental period (*e.g.*, loading magnitude stepwise up to 100 N and loading duration up to 14 wks in the referred study).

Peri-implant tissue vascularization is crucial to both peri-implant bone modeling and remodeling (Cornelini *et al.*, 2001; Marco *et al.*, 2005; Leucht *et al.*, 2007). Our findings indicated that peri-implant vascularization increases and reaches its maximum 7 days post-implantation. Based on mathematical models and *in vivo* experiments, Geris and co-workers (Geris *et al.*, 2010) suggested a consistent effect of immediate loading on improving angiogenesis in the peri-implant tissues. However, according to analysis of our data, loading failed to induce significant changes in blood vessel area. A likely explanation is that not the loading, but rather the tissue micro-environment modulated the vascular characteristics of the peri-implant tissues. The implant micro-environment includes multiple variables (*e.g.*, implant design, host bone characteristics, implant surgical procedure) that can influence vascularization (Traini *et al.*, 2006) and overrule the loading effect. More research on the vascular structure of peri-implant tissues in response to loading is needed.

Endosteal callus formation was observed. However, neither immediate nor delayed loading influenced the size and bony content of the callus when compared with the unloaded implants. An increase of the callus bone content was observed from 4 to 28 days, but this was no longer seen at later time points. Other than our findings, an enlarged endosteal callus induced by immediate loading was found in a rabbit study, whereas the bone composition of the callus was not affected by loading (Slaets *et al.*, 2009). These results, in contradiction to ours, may be due to differences in the animal models and in reference area selection. Compared with rats, the rabbit displays faster skeletal adaptation and bone turnover (Pearce *et al.*, 2007), and these characteristics may contribute to a different bone response to loading. In addition, the 1,500-μm-wide reference area in the current study, compared with the 2,500-μm one in the rabbit model, excludes meaningful comparison.

Studies support the notion that the mechanical environment affects cell gene expression adjacent to implants (Kokkinos *et al.*, 2009; Vandamme *et al.*, 2011). High strains have been recorded in the bone surrounding the implant neck (De Smet *et al.*, 2008). Hence, the tissue from this region was collected for molecular analysis. The results of the current study demonstrated that immediate implant loading up-regulated *Runx2*, a key regulator of osteoblastogenesis (Datta *et al.*, 2008). Likewise, delayed implant loading promoted *Runx2* expression, with an additional up-regulation of *Opg* (anti-osteoclastic marker) and a depressed *RANKL/Opg* ratio. Bone remodeling is tightly controlled by *RANKL* and *Opg*, and the ratio of *RANKL/Opg* is considered a good marker for bone resorption (Boyce and Xing, 2008). It has been demonstrated that excessive micro-motion at the bone-implant-interface – a key determinant in biological implant failure – can promote *RANKL* and inhibit *Opg*, thereby inducing an accelerated peri-implant bone resorption (Stadelmann *et al.*, 2008). In contrast to this excessive micro-motion, the mechanical loading exerted on the implant in the present study displayed a beneficial effect at the molecular level. Moreover, this anabolic potential was found to depend on the timing of application.

The choice of the rat model presents a study limitation, since rats lack the Haversian bone system. Haversian remodeling is thought to be an adaptation to repair micro-cracks or prevent/stop micro-crack propagation (Pearson and Lieberman, 2004). Available studies report that loading elevates Haversian remodeling rates (*e.g.*, Lee *et al.*, 2002; Voide *et al.*, 2011). Therefore, the response of

loading on intracortical peri-implant bone activity is an exciting research track to be explored in appropriate animal models.

In conclusion, controlled moderate loading restrains neither the establishment nor the maintenance of implant osseointegration and peri-implant tissue remodeling. Enhanced osseointegration can be expected when loading is initiated immediately after insertion. Tissue-level observations of peri-implant interfacial tissues could not detect an effect of loading on bone (re)modeling and vascularization. However, gene expression changes in the interfacial tissues in response to loading were observed, supporting the need for further exploration of the mechanisms underlying implant mechanobiology.

Acknowledgments

The authors acknowledge N. Smets and K. Moermans (Laboratory of Experimental Medicine and Endocrinology, KU Leuven) for their guidance on molecular biology and histology. Sincere gratitude is expressed to D. Lin (Leuven Biostatistics and Statistical Bioinformatics Centre, KU Leuven).

Article Notes

- A supplemental appendix to this article is published electronically only at http://jdr.sagepub.com/supplemental.
- This work was supported by the Research Council KU Leuven (OT/07/059)] and by the Research Foundation - Flanders (G.0500.08 and G.0982.11 to FWO).
- The authors declare no potential conflicts of interest with respect to the authorship and/or publication of this article.

- Received September 19, 2013.
- Revision received December 3, 2013.
- Accepted December 3, 2013.

References

1. Boyce BF, Xing L *(2008). Functions of RANKL/RANK/OPG in bone modeling and remodeling. Arch Biochem Biophys 473:139-146.*

2. Cornelini R, Artese L, Rubini C, Fioroni M, Ferrero G, Santinelli A, et al*. (2001). Vascular endothelial growth factor and microvessel density around healthy and failing dental implants. Int J Oral Maxillofac Implants 16:389-393.*

3. Datta HK, Ng WF, Walker JA, Tuck SP, Varanasi SS *(2008). The cell biology of bone metabolism. J Clin Pathol 61:577-587.*

4.

De Smet E, Jaecques S, Vandamme K, Vander Sloten J, Naert I *(2005). Positive effect of early loading on implant stability in the bi-cortical guinea-pig model. Clin Oral Implants Res 16:402-407.*

5.

De Smet E, Jaecques SV, Wevers M, Jansen JA, Jacobs R, Sloten JV, et al*. (2006). Effect of controlled early implant loading on bone healing and bone mass in guinea pigs, as assessed by micro-CT and histology. Eur J Oral Sci 114:232-242.*

6.

De Smet E, Jaecques SV, Jansen JJ, Walboomers F, Vander Sloten J, Naert I *(2008). Effect of strain at low-frequency loading on peri-implant bone (re)modelling: a guinea-pig experimental study. Clin Oral Implants Res 19:733-739.*

7.

Duyck J, Vandamme K, Geris L, Van Oosterwyck H, De Cooman M, Vandersloten J, et al*. (2006). The influence of micro-motion on the tissue differentiation around immediately loaded cylindrical turned titanium implants. Arch Oral Biol 51:1-9.*

8.

Duyck J, Slaets E, Sasaguri K, Vandamme K, Naert I *(2007). Effect of intermittent loading and surface roughness on peri-implant bone formation in a bone chamber model. J Clin Periodontol 34:998-1006.*

9.

Esposito M, Grusovin MG, Achille H, Coulthard P, Worthington HV *(2009). Interventions for replacing missing teeth: different times for loading dental implants. Cochrane Database Syst Rev 1:CD003878.*

10.

Geris L, Vandamme K, Naert I, Vander Sloten J, Van Oosterwyck H, Duyck J *(2010). Mechanical loading affects angiogenesis and osteogenesis in an in vivo bone chamber: a modeling study. Tissue Eng Part A 16:3353-3361.*

11.

Kokkinos PA, Zarkadis IK, Kletsas D, Deligianni DD *(2009). Effects of physiological mechanical strains on the release of growth factors and the expression of differentiation marker genes in human osteoblasts growing on Ti-6Al-4V. J Biomed Mater Res A 90:387-395.*

12.

Lee KC, Maxwell A, Lanyon LE *(2002). Validation of a technique for studying functional adaptation of the mouse ulna in response to mechanical loading. Bone 31:407-412.*

13.

Leucht P, Kim JB, Wazen R, Currey JA, Nanci A, Brunski JB, et al*. (2007). Effect of mechanical stimuli on skeletal regeneration around implants. Bone 40:919-930.*

14.

Marco F, Milena F, Gianluca G, Vittoria O *(2005). Peri-implant osteogenesis in health and osteoporosis. Micron 36:630-644.*

15.

Mertens C, Steveling HG *(2011). Early and immediate loading of titanium implants with fluoride-modified surfaces: results of 5-year prospective study. Clin Oral Implants Res 22:1354-1360.*

16.

Pearce AI, Richards RG, Milz S, Schneider E, Pearce SG *(2007). Animal models for implant biomaterial research in bone: a review. Eur Cell Mater 13:1-10.*

17.

Pearson OM, Lieberman DE *(2004). The aging of Wolff's "law": ontogeny and responses to mechanical loading in cortical bone. Am J Phys Anthropol 39(Suppl):63-99.*

18.

Sasaki H, Koyama S, Yokoyama M, Yamaguchi K, Itoh M, Sasaki K *(2008). Bone metabolic activity around dental implants under loading observed using bone scintigraphy. Int J Oral Maxillofac Implants 23:827-834.*

19.

Slaets E, Carmeliet G, Naert I, Duyck J *(2006). Early cellular responses in cortical bone healing around unloaded titanium implants: an animal study. J Periodontol 77:1015-1024.*

20.

Slaets E, Carmeliet G, Naert I, Duyck J *(2007). Early trabecular bone healing around titanium implants: a histologic study in rabbits. J Periodontol 78:510-517.*

21.

Slaets E, Naert I, Carmeliet G, Duyck J *(2009). Early cortical bone healing around loaded titanium implants: a histological study in the rabbit. Clin Oral Implants Res 20:126-134.*

22.

Stadelmann VA, Terrier A, Pioletti DP *(2008). Microstimulation at the bone-implant interface upregulates osteoclast activation pathways. Bone 42:358-364.*

23.

Traini T, Assenza B, San Roman F, Thams U, Caputi S, Piattelli A *(2006). Bone microvascular pattern around loaded dental implants in a canine model. Clin Oral Investig 10:151-156.*

24.

Vandamme K, Naert I, Geris L, Vander Sloten J, Puers R, Duyck J *(2007). The effect of micro-motion on the tissue response around immediately loaded roughened titanium implants in the rabbit. Eur J Oral Sci 115:21-29 (published erratum in Eur J Oral Sci 115:167, 2007).*

25.

Vandamme K, Naert I, Vander Sloten J, Puers R, Duyck J *(2008). Effect of implant surface roughness and loading on peri-implant bone formation. J Periodontol 79:150-157.*

26.

Vandamme K, Holy X, Bensidhoum M, Logeart-Avramoglou D, Naert IE, Duyck JA, et al*. (2011). In vivo molecular evidence of delayed titanium implant osseointegration in compromised bone. Biomaterials 32:3547-3554.*

27.

Voide R, Schneider P, Stauber M, van Lenthe GH, Stampanoni M, Müller R *(2011). The importance of murine cortical bone microstructure for microcrack initiation and propagation. Bone 49:1186-1193.*

28.

Wiskott HW, Cugnoni J, Scherrer SS, Ammann P, Botsis J, Belser UC*(2008). Bone reactions to controlled loading of endosseous implants: a pilot study. Clin Oral Implants Res 19:1093–1102.*